MODELING CO_2-DRIVEN CEMENT ALTERATION AT WELL-CAPROCK INTERFACE

Frederic Wertz[a]*, Fabrizio Gherardi[a,b], Philippe Blanc[a], Anne-Gaëlle Bader[a], Antonin Fabbri[a,c]

[a] BRGM, 3 Avenue Guillemin, F-45060 Orléans, Cedex 2, France
[b] LE STUDIUM, Loire Valley Institute for Advanced Studies, Orléans & Tours, France
[c] DGCB, ENTPE, 3 Rue Maurice Audin, F- 69518 Vaulx-en-Velin Cedex, France
e-mail: f.wertz@brgm.fr

ABSTRACT

In this paper, we report on the development of a geochemical model for wellbore cement-caprock–reservoir interfaces. This model predicts the mechanisms of cement chemical alteration due to its interaction with acid brine after the injection of supercritical CO_2 within reservoir rock. Numerical outputs indicate that at the well-reservoir interface, the intrusion into the cement paste of acid brine accompanied by aqueous CO_2 transforms portlandite and CSH into calcite and hydrated Si-gel quasi-instantaneously, leading to a slight but moderate porosity decrease. Conversely, at the well-caprock interface, portlandite dissolves, and its released Ca^{2+} ions migrate towards the caprock, where they eventually combine with slowly diffusing aqueous CO_2 to form calcite until the porosity collapses at the interface. This can significantly affect the behavior of the storage reservoir sealing. Finally, we develop a time-space characterization of the system, enhancing the main chemical mechanisms, with a future export to a geomechanical model in mind.

INTRODUCTION

The long-term safety of CO_2 geological storage (CCS) depends on the stability of the reservoir and on a proper assessment of CO_2 leakage and fluid displacement. Particular attention must be paid to the injection wellbore as a human-made discontinuity of the geological medium, especially the caprock. In addition, the chemical and mechanical integrity of the well-reservoir-caprock cement sealing must be ensured for the entire lifetime of the CCS project.

CO_2 geological storage has been quite intensively investigated in the past few years, using experimental, analytical or numerical approaches. For example, within the SACROC unit in Texas, Carey et al. (2007) studied Portland cement cores of a 55-year-old oil well exposed to CO_2 flow for ~30 years. They found that, although the integrity and the structure of the cement survived, casing-cement and cement-shale interfaces were heavily carbonated, and even the caprock showed a disturbed zone called "shale-fragment-zone" (SFZ). These are evidence of high reactivity at the cement edges, where decalcification of the C-S-H phases occurs, calcite precipitates, and even amorphous silica may be mobilized into the SFZ.

In addition, Kutchko et al. (2007) conducted lab-experiments of well cement degradation by CO_2-rich brine under geological (P, T) conditions. They proposed a degradation mechanism for portlandite. Indeed CO_2-rich acid brine dissolves portlandite $Ca(OH)_2$ and precipitates calcite $CaCO_3$. The fully carbonated zone is eventually dissolved by the unbuffered brine (pH~2.9), leading to a very porous silica material. Huet et al. (2010) confirmed these mechanisms by a benchmarked model of class-H-cement in CO_2-saturated water (pH~3.7). However, they identified the need of a better porosity-diffusivity coupling law. Recently, Gherardi et al. (2012) modeled the long-term (1000-year) geochemical evolution of cement from an idealized abandoned well in the Paris Basin, accounting for mutual interactions with adjacent caprock and reservoir domain. Because of the involved timescale, crystallized phases were predominantly involved in their calculations.

The present work aims to establish the main degradation mechanisms at the very thin interface between well and caprock for short space and time scales. To this end, we performed numerical simulations to simulate the short-term degradation of a newly built class-G-cement injection well, by CO_2-acidified brine, at the well-reservoir and well-caprock interfaces. Indeed, we aim at modeling the upward propa-

gation of the CO_2-disturbed cement zone from the reservoir to the caprock interface.

The idea is to reproduce and scale up (on a 3D well geometry) the cement degradation processes observed by Jobard et al. (2012) in laboratory experiments. Indeed, batch reactions of cement-surrounded shales in CO_2 solution over 30 and 60 days showed a highly carbonated interface between cement and shales. Cement even cracks sometimes, due to the shale volume increase. Diffusion is the only transport process considered here.

We also conducted a sensitivity analysis related to the influence of this particular factor with respect to kinetics rates, since these two processes are competing to drive the cement degradation propagation. Mineral dissolution and precipitation, as well as pH propagation, are carefully checked in order to characterize the main cement-alteration mechanisms. Porosity evolution has been paid special attention, since it can be used as a state variable for a further mechanical study on well cement failure risk (Fabbri et al., 2009).

The present work begins with a description of the system (well-reservoir-caprock). Then, the modeling scenarios are presented, including the different hypotheses concerning the effective diffusion in the cement. Presented results support a vertical and lateral scheme for cement-degradation propagation, which we discuss in light of the undertaken sensitivity analysis.

GEOCHEMICAL BACKGROUND

In this paper, we consider a newly built CO_2 injection well that starts operation within a carbonated reservoir, capped by shales, similar to the Dogger and Callovo-Oxfordian formations of the Paris Basin (Rojas et al., 1989). According to previously reported work, the injected supercritical CO_2 will partially dissolve and acidify the brine. Before the well surroundings are totally dried up, CO_2-rich brine will have already reacted with hydrated cement minerals and modified the well-reservoir interface. This degradation scheme then propagates along the well-caprock interface. The present work reports some year-long 3D-centimeter-scale simulations that aim at parameterizing the chemical intensity and spatial propagation of the cement degradation, with respect to the cement diffusivity parameters—based on laboratory experiments undertaken by Jobard et al. (2012)—and illustrates some upscaling effects.

Solutions composition

The geochemical calculations are performed in the chemical system SiO_2-Al_2O_3-Fe_2O_3-FeO-MgO-CaO-K_2O-Na_2O-SrO-CO_2-SO_4-H_2O. It includes minerals phases, aqueous phases, and gases. Different initial conditions are retained, depending on the geochemical domains. The pore solution of the caprock is assumed to be in equilibrium with its constituting minerals (illite, quartz, calcite, montmorillonite, chamosite, dolomite, celestite), following the approach of Gaucher et al. (2009). Similarly, the Dogger Reservoir pore-solution composition has been generated by assuming it to be in equilibrium with illite, montmorillonite, kaolinite, quartz, calcite, dolomite, magnesite, according to mineralogical analyses provided by André et al., (2007).

Table 1. Water initial compositions before speciation

Basis species	Cement (mol/kg)	Caprock (mol/kg)	Reservoir (mol/kg)
pH	11	7	5.1
Ca^{2+}	0.27E-01	0.54E-01	0.10E+01
Mg^{2+}	0.57E-07	0.18E-01	0.10E-01
Na^{+}	0.40E+00	0.10E+00	0.38E-02
K^{+}	0.29E-01	0.80E-03	0.15E+00
Fe^{2+}	0.19E-07	0.90E-06	0.18E-01
H_4SiO_4(aq)	0.32E-04	0.19E-03	0.11E-03
Al^{3+}	0.36E-04	0.41E-06	0.29E-02
Cl^{-}	0.43E+00	0.24E+00	0.35E-08
HCO_3^{-}	0.35E-04	0.23E-03	0.23E+00
SO_4^{2-}	0.90E-02	0.45E-02	0.11E+01
Sr^{2+}	1.00E-10	0.14E-02	0.30E-05

The solution was then acidified with gaseous CO_2 at 180 bar pressure, but still buffered by carbonates. After an initial time period to reach geochemical equilibrium, the respective values of pH are 7 for the caprock and 5.1 for the initially CO_2-acidified reservoir solutions. The cement initial pore solution is eventually calculated by assuming the equilibrium with the minerals portlandite, CSH, katoite, ettringite,

C3FH6, hydrotalcite, and calcite, leading to an initial geochemical equilibrium with pH 11. The resulting solution compositions are reported in Table 1.

Cement Material

Class-G cement involves different mineral phases bearing various elements (Ca, Si, Al, S, Mg, Fe, C, Na, K). Its mineral composition is described by Marty et al. (2009).

Table 2. Cement mineral composition

Cement	Formula	% Vol
CSH1.6	$Ca_{1.6}SiO_{3.6}$:2.58H_2O	38.1
Portlandite	$Ca(OH)_2$	26.1
Ettringite	$Ca_6Al_2(SO_4)_3(OH)_{12}$:26$H_2O$	13.8
Katoite-Si	$Ca_3Al_2SiO_4(OH)_8$	10.5
C3FH6	$Ca_3Fe_2(OH)_{12}$	5.5
Hydrotalcite	$Mg_4Al_2O_7$:10H_2O	5.4
Calcite	$CaCO_3$	0.6

Reservoir and caprock assemblages

Similarly to Gherardi et al. (2012), the reservoir and caprock mineral compositions and proportions are based on the Paris Basin example: Dogger and Callovo-Oxfordian formations, with minerals given by Gaucher et al., (2009). Table 3 gives the mineral composition assumed in these simulations, before and after the CO_2 acidification stage.

Table 3. Cement mineral composition

Mineral	Acidified Dogger (%Vol)	Shales (% Vol)
Calcite	77.5%	14.0%
Dolomite	10.2%	11.0%
Illite-Mg	0.1%	42.3%
Quartz	-	24.0%
Mg-Montm-Na	5.8%	6.0%
Siderite	4.1%	-
Kaolinite	2.0%	-
Magnesite	0.3%	-
Pyrite	-	1.0%
Chamosite	-	1.0%
Celestite	-	0.7%

MODELING APPROACH

Geochemical and physical parameters

To simulate the interactions occurring at the well-reservoir-caprock interface, we developed a simplified conceptual model that assumes the absence of advective flow between the storage reservoir, the caprock, and the well-cement. Aqueous conditions are then assumed to predominate over the entire simulated period, together with transport of dissolved species by molecular diffusion. During the simulations, temperature and pressure were held constant at 75°C and 180 bar, according to the present-day reservoir conditions (André et al., 2007). Since the focus of our modeling exercise was to investigate the very-short-term geochemical behavior of the injection wellbore cement, maximum simulation times were fixed at 365 days, in order to extrapolate from the 30-day experiment undertaken by Jobard et al., (2012). Local equilibrium is based on the thermodynamic database "Thermoddem" (Blanc et al., 2012) developed at the BRGM. The interactions occurring at the reservoir-caprock-cement interface were simulated with the TOUGHREACT simulator (Xu et al., 2004). A kinetic law based on Transition State Theory (Lasaga, 1981) is implemented in the code. Table 4 summarizes different kinetic coefficients used in the simulations.

Table 4. Kinetic coefficients

k25 is the kinetic constant at 25°C, EA the activation energy, n the degree of the additional mechanism (H^+ or HCO_3^-), S the reactive surface of the material.

Mineral	k25 mol/m^2/s	EA kJ/mol	n	S m^2/g
Portlandite[1]	2.18E-08	74.9		0.154
acid mech	8.04E-04	74.9	0.6	
CSH 1.6[2,3]	1.6E-18			2.0
acid mech	5.94E-08		0.275	
Katoite[2,3]	1.6E-18			0.057
acid mech	5.94E-08		0.275	
Hydrotalcite[2,3]	1.6E-18			0.1
acid mech	5.94E-08		0.275	
Ettringite[3]	1.14E-12			0.098
Calcite[4]	1.55E-06	23.5		0.026
acid mech	5.0E-01	14.4	1	
carb mech	6.58E-03	56.1	1.982	
Magnesite[4]	4.47E-10	63		0.026
acid mech	4.37E-05	19	1	

[1] Gali et al. 2001, [2] Schweizer 1999, [3] Baur et al. 2004, [4] Palandri and Kharaka 2004

The porosity Φ is initially 28% in the cement, 20% in the reservoir, 14.4% in the caprock. The diffusion coefficient D is set to that in water for the HCO_3^- ion, whose mobility has been intensively investigated. In our case, we have retained

the value provided by Tamini et al. (1994), where D_{HCO3-} = 6.58×10^{-9} m^2/s at 75°C. A constant Deff=10^{-10} m^2 is assumed from the carbonation experiments reported in Fabbri et al. (2009), by considering $\Phi = \Phi_0$ and $\tau_{cement} = 0.05$. For caprock and reservoir zones, we have considered a faster diffusion process by imposing:

$\tau_{shales} = 10x\ \tau_{cement}$, and $\tau_{reservoir} = 1.6x\ \tau_{shales}$.

Grid and Geometry

A simplified 3D axisymmetric radial model (Figure 1) was designed. The Mesh is 2 m high (1 m caprock, 1 m reservoir) and 1 m wide. Cement occupies the space between R = 0.05 m and R = 0.1 m. The model comprises of 2752 (43×64) cells sized from $2\times2mm^2$ at the interface up to $50\times50mm^2$. This spatial discretization responds to the need for properly solving steep chemical gradients near the interfaces and ensuring an adequate numerical accuracy. Numerical stability has been achieved by reducing the time step down to 8.66 s. Simulation time is about 50 days on a 2.66 GHz CPU. Boundary fixed conditions, are located 0.9 m away in radius from the cement interface, 1 m up and 1 m down from the caprock-reservoir interface. Elsewhere, no-flux conditions were set.

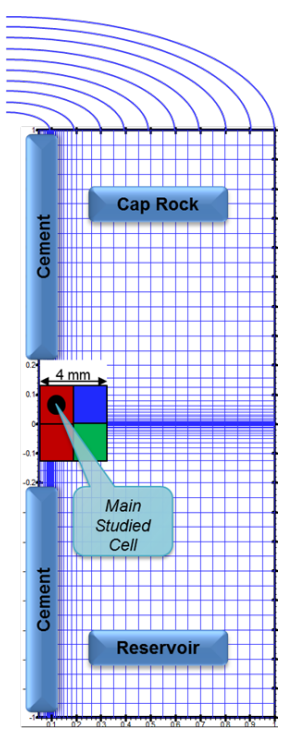

Figure 1. Geometry, Mesh and domains

RESULTS AND DISCUSSION

Identified alteration mechanisms

The first alteration mechanism was observed at the triple well-reservoir-caprock interface, related to cement acidification. Numerical outputs indicate that the pH of cement pore waters decreases with time as the CO_2-rich brines propagate from the reservoir and the caprock (Figure 2). In particular, portlandite, CSH and katoite dissolve following this order, with a decrease in pH from ~11 (near the cement material) to ~6. New phases precipitate in the cement and even at the interface with the caprock, where released ions have migrated. The final (meta)stable assemblage comprises essentially calcite, Si-Gel (hydrated silica), Al-Gel (boehmite), while the considered timescale (1 year) and kinetic rates prevented C3FH6 and ettringite from dissolving. Globally, the affected cement porosity decreases as the alteration proceeds, and is strongly dependent on the alteration stage and location.

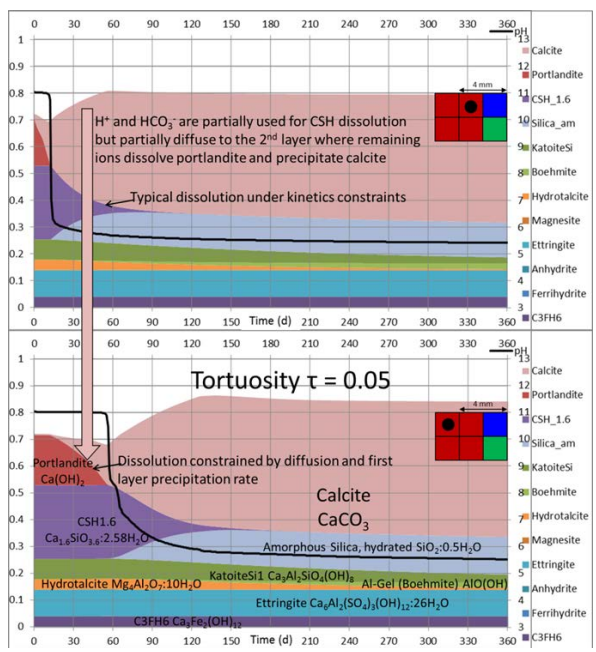

Figure 2. first and second cement layers mineral evolution over time at the interface

Concerning the Ca-bearing phases, we first notice a constant precipitation of calcite (Figure 2) due to portlandite dissolution. The controlling mechanism could be diffusion of carbonates ions. Indeed, all carbonates are trapped in the first cement numerical layer until

portlandite disappears, before calcite could precipitate in the second cement layer. This confirms that portlandite dissolution and calcite precipitation can occur in a very thin layer (less than 2 mm thickness), in spite of the ionic diffusion competition. Conversely, with respect to the Si-bearing phases, dissolution kinetics are quite slow, so that dissolving CSH does not entirely absorb the H^+ and HCO_3^- flux (by precipitating calcite). H^+ and HCO_3^- can then migrate until the second cement layer and interact with the portlandite there. Ionic mobility promotes calcite precipitation far from the location where portlandite and CSH are dissolving. Katoite (bearing Al) and hydrotalcite (bearing Mg) dissolution processes are even slower and contribute to the formation of an Al-gel (boehmite) and magnesite. Ettringite (bearing S) and C3FH6 (bearing Fe) do not dissolve during the considered timescale (1 year).

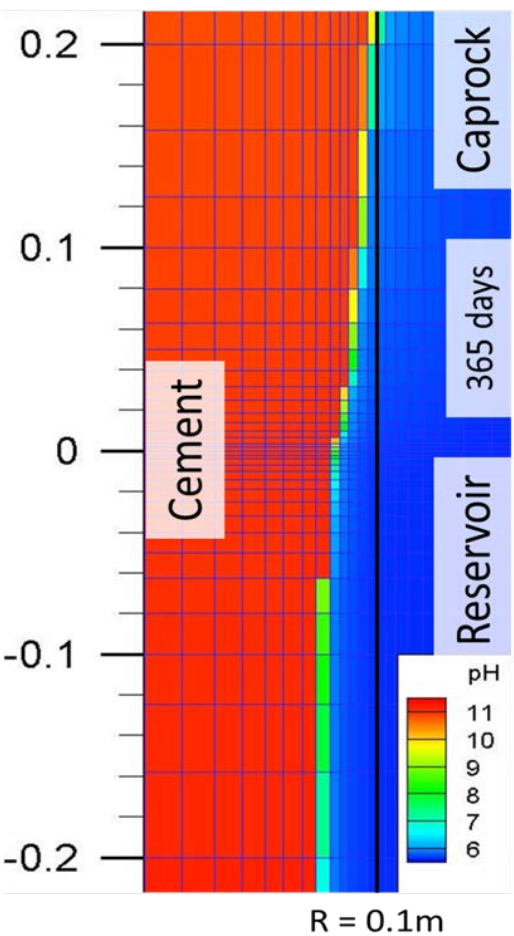

Figure 3. pH after 1 year

The second alteration mechanism concerns the upper well cement–caprock interface (Figure 3), where cement is not directly in contact with the acid brine. Ions must first diffuse vertically in the caprock. This leads to a similar degradation scheme for the cement but delayed in time. The main difference is in the creation of a porous zone (Figure 4) in the cement with a porosity-collapse counterpart in the caprock. Indeed, porosity decreases at the cement-caprock interface, starting from the triple well-reservoir-caprock interface and affecting the upper well-caprock interface by increasing the reaction time. This is due to the dissolution of portlandite and CSH while carbonates are not yet precipitating in the cement domain. Eventually, Ca^{2+} ions migrate sideways in the caprock, where they can precipitate as calcite. Experiments by Jobard et al. (2012) confirmed the highly calcified cement-shale interface.

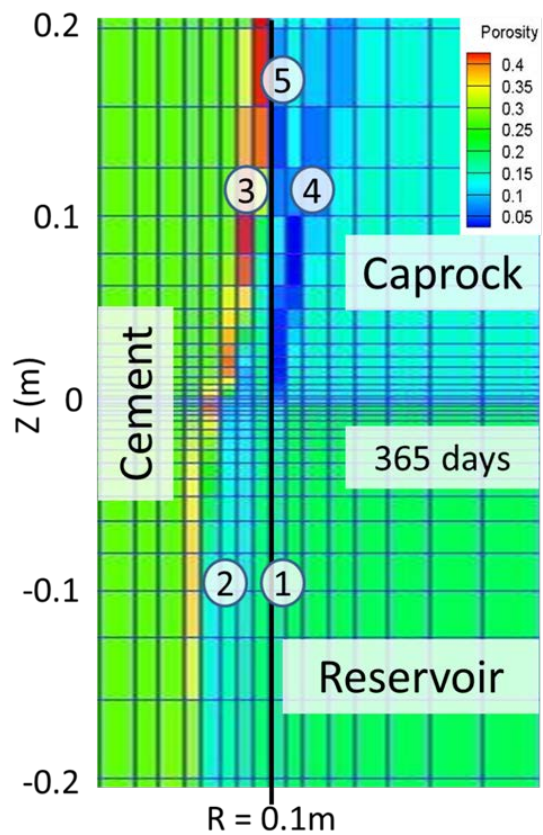

Figure 4. Porosity after 1 year

As displayed on Figure 4, the degradation and propagation mechanism follows different steps in different zones:

- Zone 1: At the well-reservoir interface, immediate dissolution of Portlandite leads to a very fast precipitation of a thin layer of calcite at the reservoir-side. This zone does not evolve further with time.
- Zone 2: Portlandite dissolution leads to a calcite precipitation front propagating radially towards the cement zone with time. This is followed by a slower rate of CSH decalcification over the entire zone, no longer buffered by portlandite. Decalcified CSH is replaced by an amorphous and hydrated silica phase. The final assemblage of silica gel and calcite implies an increase in the molar volume with respect to the portlandite + CSH association; thus, the final porosity is decreased. With time and helped by a higher diffusion rate, some Al-Gel (modeled here by an equivalent of boehmite) and magnesite can eventually precipitate near the interface.
- Zone 3: At the well-caprock interface, the neutral pH of the caprock first destabilizes portlandite. This leads to a substantial increase in porosity, while Ca^{2+} ions migrate in all directions. The thickness of this zone increases with the cement diffusion coefficient.
- Zone 4: Carbonates from the reservoir precipitate as calcite mainly on the caprock side, forming a thicker crust than at the well-reservoir interface. The thickness of this zone increases with the cement diffusion coefficient
- Zone 5: The slower dissolution of CSH delays the diffusion of silica that precipitates as an amorphous hydrated silica phase, even on the caprock side.

CONCLUSION

These simulations offer a clear representation of the different processes and mechanisms involved in cement degradation under well-geometry conditions. As in previous studies, geochemical simulation of the interface between the CO_2-injection well and the acidified reservoir shows cement mineral dissolution, accompanied by calcite precipitation in the cement porosity, as well as in the reservoir side of the interface. The degraded cement thickness reaches ~1 cm after 1 year. Portlandite is the first mineral to dissolve, with a high enough kinetic rate so that pH remains buffered. Then, CSH dissolves as soon as pH decreases, and eventually other cement minerals (katoite, hydrotalcite) also dissolve.

At the well-reservoir interface, the cement effective-diffusion parameter has an impact on the front propagation speed. Higher up, at the well-caprock interface, the degradation scheme is more complex. As the cement starts to leach due to neutral shale-water interactions before acid brines reach it, the main cement mineral portlandite start to dissolve before carbonates are supplied for calcite precipitation. Thus, the degraded zone is divided into highly porous cement and highly carbonated shales near the interface. In that region, the higher cement effective-diffusion parameter has a different impact: rather than accelerating the degradation propagation inside the well, it enlarges the cement porous zone and the carbonated shale zone.

The porosity changes in the interface model will be extracted from this study and applied to a geomechanical code that will help us deduce cement constraints and interpret interface geo-mechanical resilience.

ACKNOWLEDGMENT

This work has been supported by the French Research National Agency (ANR) through CO2 program (project INTERFACE, n° ANR-08-PCO2-006), as well as by the French Environment and Energy Management Agency (ADEME, project France Nord, Lot 7). We also would like to thank Eric Gaucher for is support and constructive review of the article during its elaboration.

REFERENCES

André, L., Audigane, P., Azaroual, M., Menjoz, A., 2007 Numerical modeling of fluid–rock chemical interactions at the supercritical CO2–liquid interface during CO2 injection into a carbonate reservoir, the Dogger aquifer (Paris Basin, France), Energy Conversion and Management 48, 1782-1797

Baur, I., Keller, P., Mavrocordatos, D., Wehrli, B., Johnson, C.A. 2004. Dissolution–precipitation behaviour of ettringite, mono-

sulfate, and calcium silicate hydrate. Cement and Concrete Research 34 (2), 341–348

Blanc, P., Lassin, A., Piantone, P., Azaroual, M., Jacquemet, N., Fabbri, A., Gaucher, E.C. 2012. Thermoddem: A geochemical database focused on low temperature water/rock interactions and waste materials. Applied Geochemistry, in press.

Carey J. W., Wigand M., Chipera S. J., Woldegabriel G., Pawar R., Lichtner P. C., Wehner S. C., Raines M. A., Guthrie Jr G. D. 2007. Analysis and performance of oil well cement with 30 years of CO2 exposure from the SACROC Unit, West Texas, USA. International Journal of Greenhouse Gas Control 1, 75 –85

Fabbri A., Corvisier J., Schubnel A., Brunet F., Goffé B., Rimmelé G., Barlet-Gouédard V. 2009. Effect of carbonation on the hydro-mechanical properties of Portland cements, Cement and Concrete Research 39, 1156–1163.

Fabbri A., Jacquemet N., Seyedi D.M. 2012 A chemo-mechanical model of oilwell cement carbonation under CO2 geological storage conditions, Cement and Concrete Research 42, 8-19

Galí S., Ayora C., Alfonso P., Tauler E., Labrador M. 2001. Kinetics of dolomite–portlandite reaction: Application to portland cement concrete. Cement and Concrete Research, 31 (6), 933-939

Gaucher, E.C., Tournassat, C., Pearson, F.J., Blanc, P., Crouzet, C., Lerouge, C., Altmann, S. 2009. A robust model for pore-water chemistry of clayrock. Geochemica et Cosmochimica Acta 73, 6470-6487.

Gherardi F., Audigane P., Gaucher E.C. 2012. Predicting long-term geochemical alteration of wellbore cement in a generic geological CO2 confinement site: Tackling a difficult reactive transport modeling challenge. Journal of Hydrology 420–421, 340–359

Huet B. M., Prevost J. H., Scherer G.W. 2010. Quantitative reactive transport modeling of Portland cement in CO2-saturated water, International Journal of Greenhouse Gas Control 4, 561–574

Jobard E., Sterpenich, J., Pironon J., Corvisier J., Randi A. 2012: Experimental modelling of the caprock/cement interface behaviour at high temperature and in presence of high pressure of CO2: The "Sandwich" experiment. To be submitted at the International Journal of Greenhouse Gas Control

Kutchko B.G., Strazisar B.R., Dzombak D.A., Lowry G.W., Thaulow N. 2007. Degradation of Well Cement by CO2 under Geologic Sequestration Conditions. Environmental Science and Technology 41, 4787-4792

Lasaga, A.C. 1981. Rate laws in chemical reactions. In: Lasaga, A.C., Kirkpatrick, R.J., (Eds.), Kinetics of Geochemical Processes. Reviews in Mineralogy 8, 135–169

Palandri J.L. and Kharaka Y.K. 2004. A compilation of rate parameters of water-mineral interaction kinetics for application to geochemical modelling. U.S. Geological Survey Report 2004-1068

Rojas, J., Giot, D., Le Nindre, Y.M., Criaud, A., Fouillac, C., Brach, M., Menjoz, A., Martin, J.-C., Lambert, M., 1989. Caractérisation et modélisation du réservoir géothermique du Dogger, Bassin Parisien, France. Rapport final CCE, EN 3G-0046-F(CD), BRGM R 30 IRG SGN 89.

Schweizer Ch. R. 1999. Calciumsilikathydrat-Mineralien. Lösungskinetik und ihr Einfluss auf das Auswaschverhalten von Substanzen aus einer Ablagerung mit Rückständen aus Müllverbrennungsanlagen. PhD thesis, dipl. Chem. Universität Basel, Zürich und Dübendorf

Tamini A., Rinker E.B., Sandall O.C., 1994. Diffusion Coefficients for Hydrogen Sulfide, Carbon Dioxide, and Nitrous Oxide in Water over the Temperature Range 293-368 K. Journal of Chemical Engineering Data 39, 330-332

Xu H., Sonnenthal E. L., Spycher N., Pruess K. 2004. TOUGHREACT user's guide: a simulation program for nonisothermal multiphase reactive geochemical transport in variably saturated geologic media, Lawrence Berkeley National Laboratory, Berkeley, California, Report LBNL-55460.